

Dynamic Mechanical Study of Four Amorphous Polymers around and above the Glass Transition. Breakdown of the Time-Temperature Superposition Principle in the Frame of the Coupling Model[†]

A. Alegría,* E. Macho,[‡] and J. Colmenero

Departamento de Física de Materiales, Facultad de Química, Universidad del País Vasco, Apartado 1072, E-20080 San Sebastián, Spain

Received January 25, 1991; Revised Manuscript Received April 23, 1991

ABSTRACT: The dynamic mechanical behavior of four structurally related amorphous polymers has been investigated around and above their glass transition. In this temperature range two dispersion processes associated with segmental motion and the terminal zone, respectively, have been well resolved. However, the time-temperature superposition principle cannot be applied simultaneously to these processes. Segmental motion and terminal zone processes have been described in terms of the Havriliak-Negami relaxation function. We have also found that the time domain Fourier transform of those H-N behaviors can be well described by means of stretched exponential functions, and therefore it is possible to characterize process by means of a single shape parameter, β . The so-obtained β parameters for the two dispersion are related to the corresponding apparent activation energies in the way expected by the coupling model when a common microscopic friction coefficient is assumed to control both processes.

Introduction

The dynamics in polymer melts has been a field of great scientific interest for several years.¹⁻⁵ This interest arises mainly from the fact that a polymer melt presents two different dynamics, each of them having a different characteristic time scale and nature.²⁻⁶ It is well established that the fastest of these two dynamics is associated with segmental motions of small parts of the main chain, and then it depends strongly on the local chemical structure of the polymer. This kind of motion is present in all polymeric systems, and its characteristic time scale is nearly independent of molecular weight. The main features of this process are similar to those observed in the dynamical behavior of low molecular weight glass-forming liquids. However, the slowest of the two dynamics mentioned above is a specific feature of the polymeric systems, and it is controlled by the translational diffusion of the chain along its own contour and therefore depends mainly on the topological features of the polymer chain. The characteristic time scale corresponding to this process is strongly dependent on molecular weight; the higher the molecular weight of the polymer, the greater the difference between the time scale characteristics of the two dynamics.

The presence of the two different dynamical regimes on a given polymer melt can be checked by studying its dynamic mechanical response.⁶ The dynamic mechanical behavior around and above the glass transition of high molecular weight glassy polymers shows two well-resolved dispersion regions, each of them related to one of the two different dynamical regimes mentioned above. The dispersion region called the primary α -relaxation occurs in the glass transition range, and it is related to the segmental motion (fast dynamics). The other one is usually detected at temperatures well above the glass-transition range; i.e., it corresponds to the slowest process, and it is known as a terminal zone relaxation. This latter dispersion process is the precursor to the Newtonian flow corresponding to

an ideal fluid that may only be reached at very high temperatures.

Standard characterization of the dynamic mechanical behavior of polymers is usually performed by studying the real and imaginary components of the modulus or the compliance as a function of both frequency and temperature.⁶⁻⁸ The experimental data obtained by this method usually extend over a wide temperature range but involve in general only a few decades in frequency.⁸ However, the application of the time-temperature superposition principle allows us to extend the mechanical behavior over a wider reduced frequency range.⁶ The time-temperature superposition principle assumes that the temperature only shifts the relaxation on the time scale but does not change the shape or nature of the relaxation process. In some cases this assumption is not actually true, so that the time-temperature superposition principle must be carefully used.⁹ In this sense, it has been clearly shown that in many cases there is a clear breakdown of the superposition principle just in the range of the glass-rubber transition.⁹

In general, the two mechanical dispersion processes observed on polymer melts extend over several decades in frequency so they cannot be described as single Debye relaxations. Such a behavior is commonly explained by the assumption of a continuous distribution of Debye-like relaxation processes (relaxation time spectrum) associated to each particular dynamics. Following this idea each individual relaxation time is characteristic of the behavior of a certain number of relaxing units.⁸ In this framework, the experimental behavior observed is ascribed to the superposition of the different elementary processes. There are several reasons to accept the existence of such a distribution, taking into account the structural features of the polymers (molecular weight distribution as an example). However, as far as we know, a definitive link between the structural properties and the experimentally found relaxation time distribution has not been established up to date.

Another alternative explanation for the broad dispersion experimentally observed can be found in the frame of the coupling model.^{10,11} This theoretical model is based on

[†] Dedicated to Prof. G. M. Guzmán on the occasion of his appointment as Professor Emeritus.

[‡] Departamento de Física Aplicada I, ETSII, Universidad del País Vasco, Bilbao, Spain.

the dynamics of complex correlated systems, and it studies the coupling of a primitive relaxation mode to a complex system. In this framework, motions of the fundamental mode on small spatial scales are well-defined, but, as the relaxation develops, they encounter cooperativity and complexity. Thus, complexity of the system results in a slowing down of the process. In the coupling model scheme, the relaxation rate of the fundamental mode becomes modified in a time-dependent factor $(\omega_c t)^{-n}$, where ω_c is a frequency that characterizes the complexity of the system, and for polymers it is expected to be on the order of 10^{10} s^{-1} . The index n is then a measure of the coupling strength of the fundamental mode to the complex system. The main predictions of coupling model are as follows:

(i) a stretched exponential behavior for the time decay function $\varphi(t)$

$$\varphi(t) = \exp[-(t/\tau)^\beta] \quad \beta = 1 - n \quad (1)$$

(ii) a power law for the relationship between the fundamental time scale τ_f and the observed one τ

$$\tau \propto (\tau_f)^{1/\beta} \quad (2)$$

Equation 1 takes into account the non-Debye character of the relaxation processes usually observed,^{6,8} while eq 2 displays the relationship between the fundamental time scale and the observed one.

In spite of the different molecular origin of the two dispersion processes taking place in polymer melts, both are related to the main-chain dynamics although involving two different length scales. This fact has led several authors to look for some relationship between the two dynamics.¹²⁻¹⁵ In this sense, Ngai's coupling model considers that these dynamics are associated with two different coupling indexes, whereas the fundamental motion is similar. The different values of the coupling indexes are related to the differences in the geometry of the main motion associated with each dynamics (i.e., segmental motion and diffusional translation). With this main idea, the model assumes that the value of the coupling index in the terminal zone should be similar for all the linear polymers that have been found experimentally.^{11,12} Moreover, recent Monte Carlo and molecular dynamics computer simulations appear to confirm these results.¹⁶ This fact is explained by consideration of the similarity of the motion geometry in the range where the molecular motion corresponds to translational diffusion.

However, from an experimental point of view the value of the coupling index corresponding to the main-chain diffusional translation is generally found to be lower than the coupling index associated with the segmental motion in which the geometry is close to rotational diffusion. In the framework of the coupling model, the difference between the coupling indexes associated with the two dynamics can explain the differences observed in the temperature behavior of the characteristic time scales through eq 2. If a fundamental friction coefficient, $\zeta_f(T)$, is assumed to control each dynamical regime (in the sense that the fundamental relaxation rate is proportional to $\zeta_f(T)$, the experimental time scale happens to be related to this fundamental friction coefficient in the following way:

$$\tau(T) \propto [\zeta_f(T)]^{1/\beta} \quad (3)$$

By means of eq 3 a relationship between the apparent activation energy of each dispersion process and the one corresponding to the fundamental motion can be estab-

lished as

$$E_a = \frac{d \ln \tau(T)}{d(1/T)} = \frac{1}{\beta} \frac{d \ln \zeta_f(T)}{d(1/T)} \quad (4)$$

Then, if the fundamental friction coefficients $\zeta_f(T)$ controlling both dynamical regimes (segmental and terminal ones) are the same, the ratio of the corresponding apparent activation energies should be the same as the reciprocal of the ratio of the corresponding values of the β parameter, i.e.

$$E_{as}/E_{at} = \beta_T/\beta_S \quad (5)$$

where the subscripts S and T refer, respectively to the segmental and terminal dynamics. The values of E_a and β can be determined independently from experiments. Thus, the relation 5 could be considered as a test of the coupling model scheme.

In the present work, the dynamics of the polymer melt as observed from dynamic mechanical measurements are compared for four structurally related glassy polymers. The frequency dependence of the mechanical modulus in each of the two dispersion regions is obtained by applying separately to each of them the time-temperature superposition principle. Thereafter, each dispersion region is described in terms of a Havriliak-Negami-like equation.¹⁷ On the other hand, shift factors used to build the master curve allow the determination of the temperature dependence of the characteristic time scales. These temperature behaviors are compared with those obtained for the zero-shear viscosity. The results obtained are interpreted in the frame of Ngai's coupling model outlined above.

Experimental Section

Materials. Four commercial glassy polymers having the Bisphenol A residue have been investigated. They are Bisphenol A polycarbonate (PC), poly(aryl ether sulfone) (PSF), a copolymer of Bisphenol A and epichloridrine (phenoxy, PH), and a copolyester of Bisphenol A and an equimolar mixture of isophthalic and terephthalic acids (polyacrylate, PAr). All the polymers were supplied by Union Carbide.

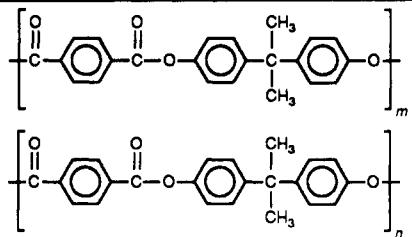
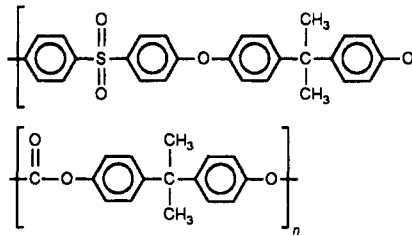
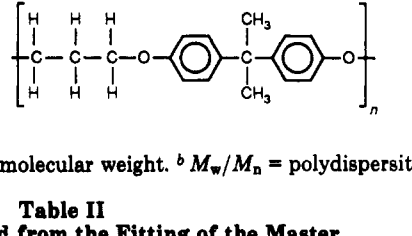
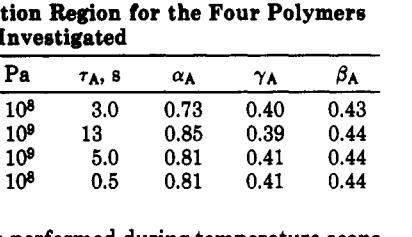
A general description of the polymers investigated in this work, including generic chemical structure and glass transition temperatures T_g , determined from the middle point of the specific heat increment in a DSC scan at a heating rate of 10 K/min, is shown in Table I.

Mechanical Measurements. A standard Polymer Laboratories DMTA apparatus operating in bending- and shear-mode was used. This instrument measures dynamic mechanical properties using either flexural deformations (bending-mode) or shear deformation (shear-mode) and delivers the real and imaginary components of the complex Young's modulus in the bending mode ($E^* = E' + iE''$) and of the complex shear modulus in the shear mode ($G^* = G' + iG''$). The frequency range covered extends from 0.1 to 100 Hz.

By means of the experimental setup described above, bending-mode measurements are adequate in the temperature range around and below the glass transition temperature range, but at temperatures above $T_g + 30 \text{ K}$ this mode of operation fails because the changes in sample geometry lead us to obtain no reliable data. In contrast, the shear mode is adequate in the temperature range from $T_g + 10$ to $T_g + 80 \text{ K}$, but around and below T_g it is not successful, leading to unrealistic low values of the modulus. Then, combining both deformation modes, we can study the dynamic modulus behavior of glassy polymers from temperatures just below T_g to about $T_g + 80 \text{ K}$.

Bending-mode measurements were performed at isothermal conditions in temperature steps of 5 K. When this experimental procedure is used, the sample remains about 1 h at each temperature during the frequency scan over the entire frequency range. For the highest temperatures where shear mode applies, this long time conduces to degradation of the sample, so shear-

Table I
General Description of the Polymers Investigated

polymer		M_n^a	M_w/M_n^b	T_g , K
PAr		21 000	2.46	466
PSF		31 000	2.02	463
PC		17 000	1.53	424
PH		25 000	3.20	370

^a M_n = number-average molecular weight. ^b M_w/M_n = polydispersity.

Table II
Parameters Obtained from the Fitting of the Master Curves in the α -Relaxation Region for the Four Polymers Investigated

	T_{ref} , K	E_{-A} , Pa	τ_A , s	α_A	γ_A	β_A
PAr	457	8.3×10^8	3.0	0.73	0.40	0.43
PSF	457	1.3×10^9	13	0.85	0.39	0.44
PC	417	1.4×10^9	5.0	0.81	0.41	0.44
PH	359	8.3×10^8	0.5	0.81	0.41	0.44

mode measurements were performed during temperature scans at a constant heating rate of 2 K/min, which avoids the degradation of the sample in the temperature range used by us.

Sample Preparation. Sheet stocks 0.6–0.8 mm thick were formed by pressing the commercial material in an air atmosphere by a Schwabenthan Polystat 200T press at 65 atm and 100 °C above the corresponding glass transition temperature. Sheets were dried under vacuum at 120 °C for 40 h. For DMTA bending-mode measurements, 12 mm \times 30 mm rectangles were cut from the sheets.

On the other hand, bands 3 mm thick and 14 mm wide were obtained in a Sieglaff McKelvey rheometer (Tinius Olsen Testing Machine Co., Inc.) 100 °C above the corresponding glass transition temperature. Shear rates were chosen so that the obtained bands were homogeneous. For DMTA shear-mode measurements, 7-mm-diameter disks were cut from the bands.

Results and Discussion

Frequency Dependence. The dynamic mechanical behavior observed is very similar for the four polymers investigated. For all of them, the two dispersion regions mentioned above, which will be called A (segmental motions) and B (terminal zone), are apparent around T_g and $T_g + 30$ K, respectively. In order to obtain the values of the relaxation parameters, master plots were constructed by the horizontal scaling of the log–log plots from the experimental data to give visually coherent master curves. Reference temperatures used for each polymer can be found in Table II for the A dispersion region and in Table III for the B dispersion region. Master plots at these reference temperatures showing E^* vs ωa_T corresponding to the A dispersion region and G^* vs ωa_T corresponding

Table III
Parameters Obtained from the Fitting of the Master Curves in the Rubber–Liquid Transition Region for the Four Polymers Investigated

	T_{ref} , K	G_{-B} , Pa	τ_B , s	α_B	γ_B	β_B
PAr	523	2.4×10^6	0.05	0.55	0.80	0.49
PSF	520	1.7×10^6	0.008	0.57	1.0	0.63
PC	463	5.5×10^5	0.1	0.71	0.85	0.64
PH	423	1.2×10^6	0.005	0.56	1.0	0.60

to the B dispersion region can be seen in Figure 1 and 2 respectively. The corresponding shift factors, a_T , have been plotted versus the reciprocal temperature in Figure 3.

As can be seen in Figures 1 and 2 both dispersion processes extend over around 7 decades in the reduced frequency scale. In both cases the superposition principle can be applied as a good approximation. Only for the lowest frequencies of the A process (the highest ones of the B process) does a high scattering of data appear. The reason for this behavior in this range of reduced frequencies is that both processes overlap in this region. This is a first indication that, although the superposition principle can be applied to each single dispersion process, the time scales associated with these dynamics behave differently with temperature. This fact is clearly shown in Figure 3. For all the polymers this shift factors corresponding to the A process vary faster with temperature than those obtained for the terminal zone.

In both regions (A and B), the dynamic mechanical behavior has been characterized by using the Havriliak–Negami equation. The existence of the two dispersion regions leads us to assume that the complex modulus can be written as

$$M^*(\omega) = M_{\infty A}[1 - \Phi_A(\omega)] + M_{\infty B}[1 - \Phi_B(\omega)] \quad (6)$$

In eq 6 M^* refers to Young's modulus (E) when the measurements were performed by using the bending deformation mode or to the shear modulus (G^*) when the shear deformation mode was chosen. $\Phi(\omega)$ is the normalized complex relaxation function that we assume to

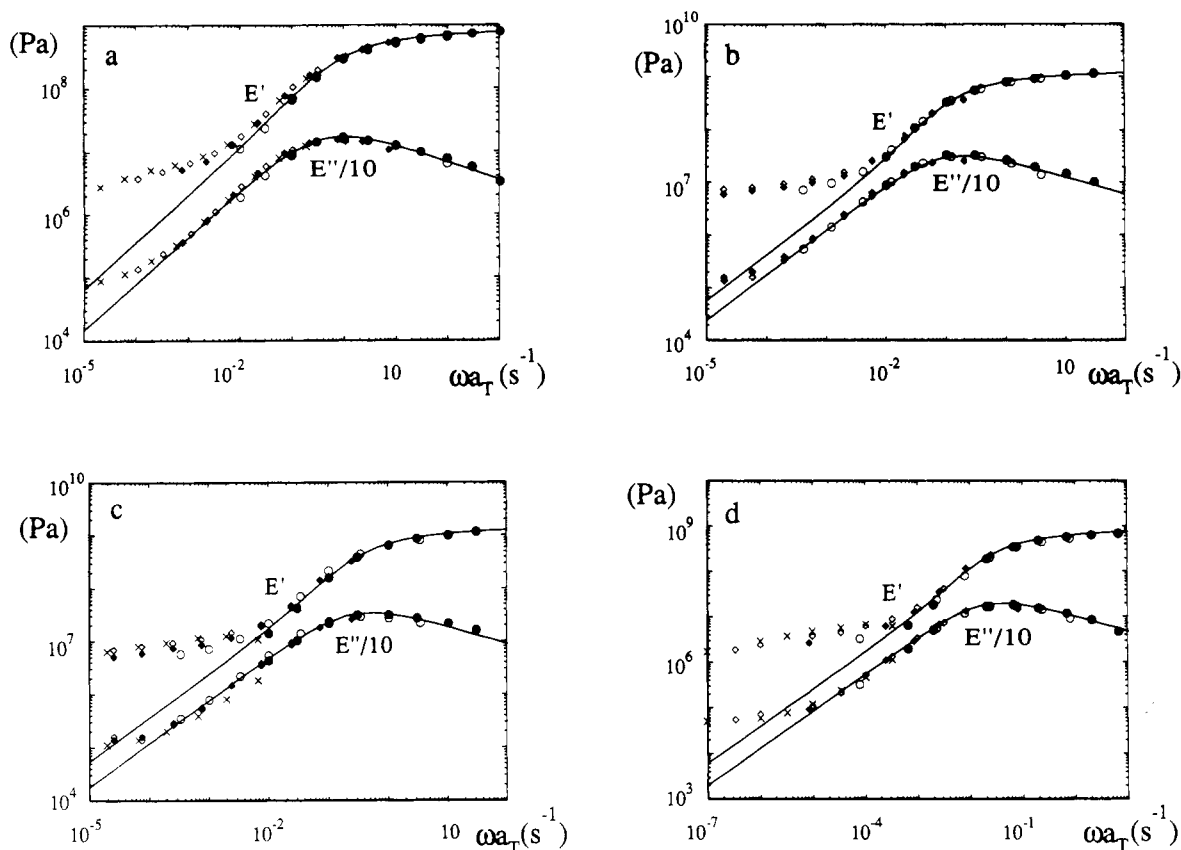


Figure 1. Complex Young's modulus reduced frequency behavior for (a) PAR (●, 452 K; ○, 457 K; ◆, 462 K; ◇, 467 K; ×, 472 K), (b) PSF (●, 452 K; ○, 457 K; ◆, 467 K; ◇, 472 K), (c) PC (●, 417 K; ○, 422 K; ◆, 427 K; ◇, 432 K; ×, 437 K), and (d) PH (●, 359 K; ○, 362 K; ◆, 365 K; ◇, 371 K; ×, 377 K).

follow a Havriliak–Negami form,¹⁷ i.e.

$$\Phi(\omega) = \frac{1}{[1 + (i\omega\tau_{HN})^\alpha]^\gamma} \quad (7)$$

Equations 6 and 7 fit the experimental behavior over the entire temperature range investigated. The values of the fitting parameters corresponding to the master curves shown in Figures 1 and 2 are shown in Table II for α -relaxation (A) and in Table III for terminal relaxation (B). The obtained fitting curves are shown in Figures 1 and 2 in comparison with the master curves built from the experimental data.

The agreement between the experimental data and the fitting curves is reasonable for each dispersion process. However, systematic differences appear in the low-frequency range of the terminal dispersion. This deviation could be due to the fact that we have used polydisperse samples. As is well-known the dispersion behavior in the terminal zone is very dependent on the molecular weight.⁶ Thus, for each polymer, the observed B process should arise from the superposition of different processes, each of them associated with a single molecular weight. Then the parameters obtained for this region would be affected by the molecular weight distribution of the sample. In this way, the expected value of the α -parameter for a monodisperse sample should be 1. Polydispersity gives us a measure of the sample deviation from the ideal monodispersity. For a monodisperse sample, polydispersity takes the value 1, while as the molecular weight distribution broadens, polydispersity increases. If the values of the α -parameter and the polydispersity are related, it should be expected that when the polydispersity value is 1 (monodisperse sample), the value of the α -parameter will be 1, and as the polydispersity increases, the α -parameter would

be lower than 1. With this argument, we can explain the low value of the α -parameter in the B process and relate it to the polydispersity of each polymer. As can be seen in Table III, PC has the highest value for this parameter as we could expect from its lowest polydispersity value (see Table I). The other three polymers have similar values but are smaller than the one corresponding to PC, as it should correspond due to their higher polydispersity values.

Nevertheless, the α -relaxation is not very dependent on molecular weight. The obtained parameters depend only on the polymer structure. In any case, the values that we obtain are not far away from the reported ones for different polymers.

It has been mentioned above that the H–N response function, which is defined in the frequency domain, corresponds to a nonexponential decay in the time domain. On the other hand, this time behavior can be described approximately by a stretched exponential functional form (eq 1). Then, the H–N response functions $\Phi_A(\omega)$ and $\Phi_B(\omega)$ previously used to describe the experimental behavior should correspond approximately to stretched exponential functions in the time domain, and therefore it is possible to obtain the values of the corresponding β exponents by fitting to stretched exponential functions the half-sided cosine Fourier transform of the imaginary part of the H–N equations $\Phi_A(\omega)$ and $\Phi_B(\omega)$ over the angular frequency ($\Phi''(\omega)/\omega$). In order to illustrate this fact, in Figure 4 we show an example of how the Fourier transform corresponding to a H–N equation behaves in time and how the stretched exponential form allows a good description of this time behavior. Values of the so-obtained β exponents for the A and B dispersion processes are shown in Tables II and III, respectively. As can be seen, the values of the

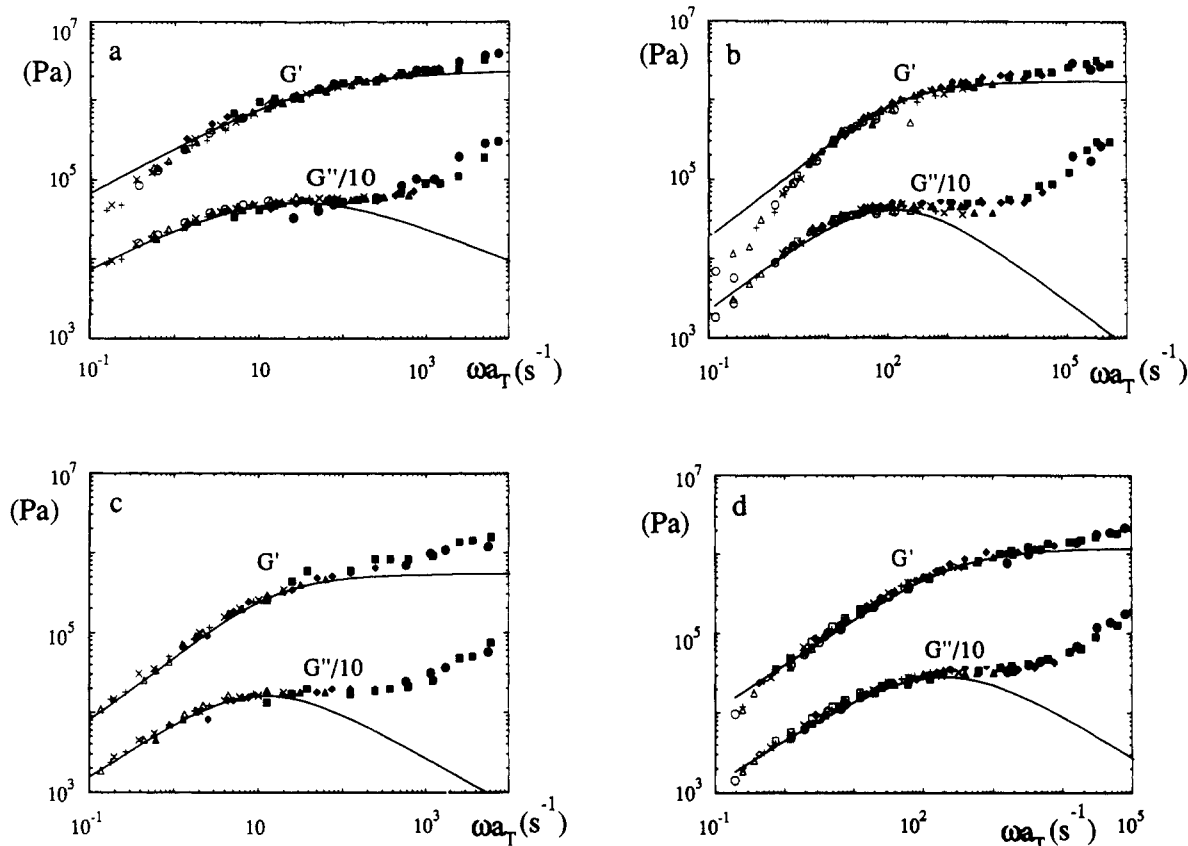


Figure 2. Complex shear modulus reduced frequency behavior for (a) PAr (●, 493 K; ■, 503 K; ◆, 513 K; ▲, 523 K; ×, 533 K; +, 543 K; △, 553 K; ○, 563 K), (b) PSF (●, 480 K; ■, 490 K; ◆, 500 K; ▲, 510 K; ×, 520 K; +, 530 K; △, 540 K; ○, 550 K; ■, 560 K), (c) PC (●, 433 K; ■, 443 K; ◆, 453 K; ▲, 463 K; ×, 473 K; +, 483 K; △, 493 K), and (d) PH (●, 383 K; ■, 393 K; ◆, 403 K; ▲, 413 K; ×, 423 K; +, 433 K; △, 443 K; ○, 453 K; ■, 563 K; ◇, 473 K).

β parameter obtained for the α -relaxation, β_A , are similar for all the polymers. The similarity in β_A values could be associated with the fact that the four polymers investigated present the rest of Bisphenol A in their repeating unit, which would control the dynamics of segmental motions. However, in the terminal zone the β values, β_B , corresponding to the studied polymers are systematically higher than the ones obtained for the α -relaxation, and moreover they scatter more. The difference between the β exponent values found for the two dispersion regions on the studied materials agrees with the results reported in the literature for different kinds of polymers.

As has been mentioned above, in the frame of the coupling model the parameter β gives a measure of the coupling between the fundamental motion and the surrounding complex medium. In this frame the differences between β values corresponding to the dispersion regions A and B can be understood in terms of the difference in the geometry of the whole motion responsible of each dispersion process, which should give rise to the different couplings between the moving unit and the neighbor units. Segmental motions corresponding to the A process are supposed to be complex. In this kind of polymer this movement involves segmental rotations that should be strongly hindered because of the presence of rigid aromatic rings in the main chain. This fact could lead to the relatively low values of the β exponent obtained. In contrast, the translational diffusion of the chain along its own contour controls the terminal zone. This corresponds to relative displacements in the backbone direction of the rigid main chains of the polymers, which would lead to a relatively low coupling among them and, as a consequence, to higher values of the β exponent in this region.

Temperature Dependence. The application of the time-temperature superposition principle assumes that in eqs 6 and 7 only the characteristic time scales τ_A and τ_B depend on temperature. Thus, the temperature dependence of the shift factors can be monitored by the temperature dependence of the corresponding characteristic time scales. In these conditions the shift factor a_T and the characteristic time scale τ are related by

$$a_T(T) = \tau(T)/\tau(T_r)$$

where T_r is the reference temperature taken to build the master curves. In this way, the shift factor and characteristic time scale behave with temperature in the same way.

In order to discuss the temperature behavior of the characteristic times scales, first, we have compared the a_T temperature behavior with zero-shear viscosity, η .¹⁸ As can be seen in Figure 3, the behavior of the characteristic time scale corresponding to the B process is in good agreement with the temperature dependence of the viscosity, showing that, as expected, the mechanisms controlling both viscosity and terminal zone dynamics are intimately related. It is well established that the temperature behavior of the viscosity, and, therefore, that of the characteristic time scale of the terminal zone, follows a non-Arrhenius behavior that, in general, can be well described by Vogel-Fulcher^{19,20} (V-F) or Williams-Landel and Ferry laws.⁶ The former can be written as

$$a_T \propto \exp\left[\frac{T_1}{T - T_0}\right] \quad (8)$$

where T_0 is the temperature at which the time scale

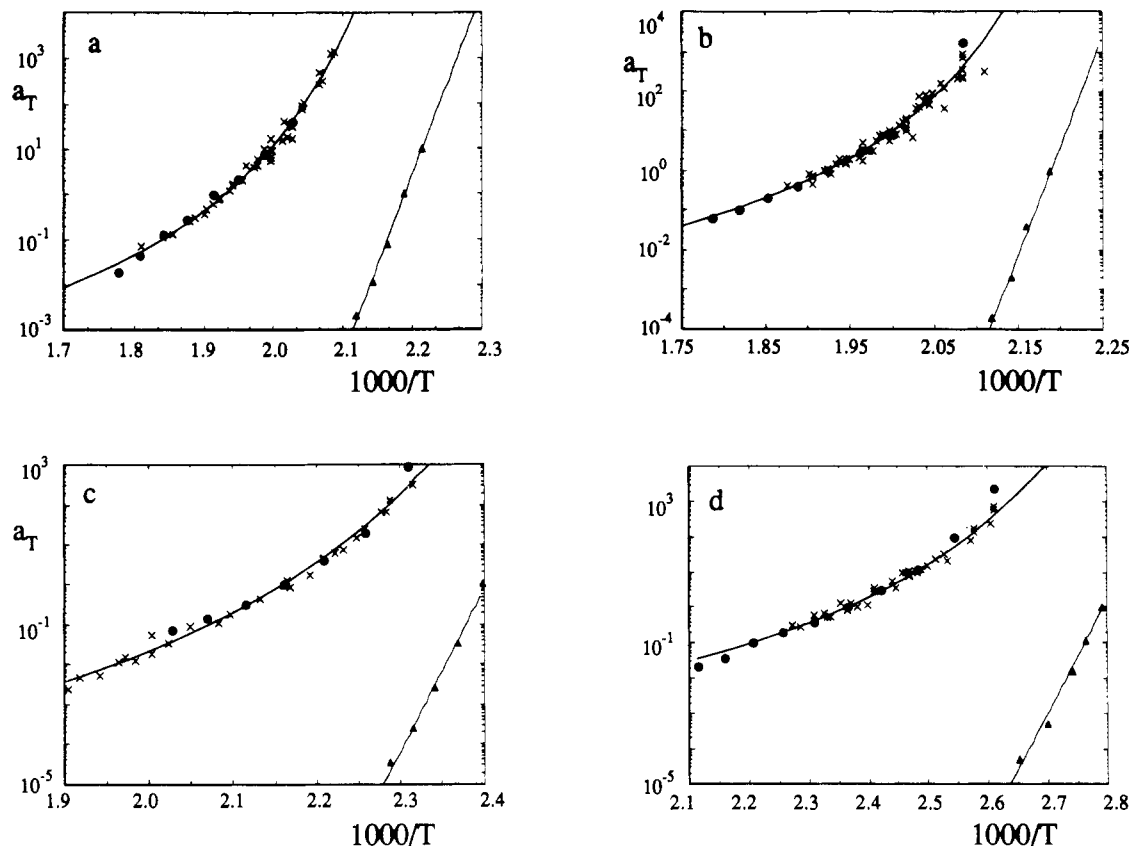


Figure 3. Arrhenius plot of the shift factor a_T , obtained from bending (Δ) or shear (\bullet) deformation modes data, and reduced Newtonian viscosity, $\eta(T)/\eta(T_{ref})$ (\times) for (a) PAr, (b) PSF, (c) PC, and (d) PH. Continuous lines are the Vogel-Fulcher fits of the viscosity data.

Table IV
Values of the V-F Parameters, T_{0B} and T_{1B} , for the Temperature Behavior of the Characteristic Time Scale Corresponding to the Terminal Dynamics and of the Apparent Activation Energies at T_g , E_{aB} , and E_{aA} , for Both Processes^a

	T_g , K	T_{0B} , K	$T_{1B} \times 10^3$, K	E_{aB} , kcal/mol	E_{aA} , kcal/mol	E_A/E_B	β_B/β_A
PAr	466	415	1.20	199	191	0.96	1.07
PSF	463	414	1.04	184	248	1.35	1.43
PC	242	349	1.78	116	185	1.60	1.45
PH	370	311	1.20	93	117	1.26	1.36

^a The reciprocal of the ratio between the corresponding β parameters is shown for comparison.

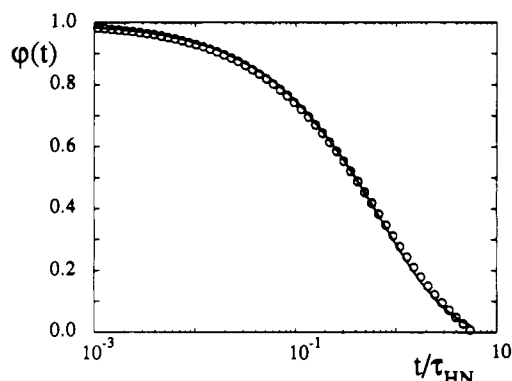


Figure 4. Comparison between the time domain response corresponding to the H-N function ($\alpha = 0.85$ and $\gamma = 0.71$), empty points, and the stretched exponential ($\tau = 0.9\tau_{HN}$ and $\beta = 0.64$), continuous line.

diverges and T_1 is an apparent activation parameter, which in the frame of free-volume theories is related to the expansion coefficient of the free volume. The continuous curves in Figure 3 represent the V-F fit for the viscosity that was reported previously.¹⁸ The values of the fitting parameters can be found in Table IV. As was discussed in the previous paper¹⁵ the values we had found for the

V-F parameters are reasonable in the free-volume framework.

As mentioned above, shift factors corresponding to the A process vary with temperature faster than the ones corresponding to the B process (see Figure 3). However, in this case, instead of the expected V-F behavior, an apparent Arrhenius-like behavior is found. Similar behavior for the temperature dependence of the shift factors near the glass transition has been reported in the literature.^{6,8} In order to account for the unphysical values of the apparent activation energies usually obtained, several explanations have been outlined. On the one hand, in some cases this behavior has been interpreted as a consequence of the fact that there is a crossover from a V-F behavior to an Arrhenius like one through the glass transition temperature.⁶ On the other hand, the temperature range covered experimentally by us for this dispersion process could not be large enough to allow a definitive answer about which of both types of temperature dependences (V-F or Arrhenius-like) applies in this case.

As mentioned above, if there is a common microscopic friction coefficient controlling the dynamics of both the segmental motion and the terminal zone, a correlation between the temperature dependence and the frequency behavior should be expected, in the frame of the coupling

model. In order to test whether or not the differences we have found for the temperature behavior of the A and B processes are correlated to the differences in the frequency behavior (different values of the β parameter), we have calculated the apparent activation energies, E_a , of both processes at T_g :

$$E_a = \frac{1}{R} \left[\frac{d \ln a_T}{d(1/T)} \right]_{T=T_g} \quad (9)$$

For the A relaxation, the glass transition temperature is located within the experimental temperature range we have measured, so in this case E_a values were obtained directly by fitting the experimental behavior to an Arrhenius law. However, for the B process T_g is always out of the temperature range experimentally covered by us, so in this case the apparent activation energy at T_g was determined using both eq 9 and the V-F law fitting the viscosity; i.e.

$$E_{aB} = \frac{T_{1B} T_g^2}{R(T_g - T_{0B})^2} \quad (10)$$

Values obtained for each polymer are shown in Table IV.

Ngai's coupling model considers the differences between the temperature behavior of the characteristic time scales as a consequence of the different coupling (different values of the β exponent) between the common fundamental motion and the surrounding media corresponding to the two processes. If these ideas apply, in our case the ratio of the values obtained for the E_a (E_{aA}/E_{aB}) will be similar to the ratio of the reciprocal of the corresponding β exponents ($\beta_A^{-1}/\beta_B^{-1}$). As can be seen in Table IV, these rates are similar within the experimental uncertainty taken as 10%.

Conclusions

The main result of this work is the successful test of the coupling model in relation to the breaking of the time-temperature superposition principle around the glass transition in polymers. In this sense, the β parameters we

have obtained for the two dispersion processes on each polymer are related to the corresponding apparent activation energies in the way expected from the coupling model when a common microscopic friction coefficient is assumed to control both processes.

Acknowledgment. We express our gratitude to K.L. Ngai for fruitful discussions. We also thank Gipuzkoako Foru Aldundia for partial financial support.

References and Notes

- (1) de Gennes, P.-G. *J. Chem. Phys.* **1971**, *55*, 572.
 - (2) Doi, M.; Edwards, S. F. *The Theory of Polymer Dynamics*; Clarendon Press: Oxford, 1986.
 - (3) Raju, V. R.; Menezes, E. V.; Marin, G.; Graessley, W. W. *Macromolecules* **1984**, *14*, 1668.
 - (4) Ngai, K. L.; Plazek, D. J. *J. Polym. Sci. Polym. Phys. Ed.* **1985**, *23*, 2159.
 - (5) Richter, D.; Farago, B.; Fetters, L. J.; Huang, J. S.; Ewen, B.; Lartigue, C. *Phys. Rev. Lett.* **1990**, *64*, 1389.
 - (6) Ferry, J. D. *Viscoelastic Properties of Solid Polymers*; John Wiley and Sons: New York, 1980.
 - (7) Ward, I. H. *Mechanical Properties of Solid Polymers*; John Wiley and Sons: New York, 1979.
 - (8) McCrum, N. G.; Read, B. E.; Williams, G. *Anelastic and Dielectric Effects in Polymeric Solids*; Wiley: London, 1967.
 - (9) Cavaille, J. Y.; Etienne, S.; Perez, J.; Monnerie, L.; Johari, G. P. *Polymer* **1986**, *27*, 549.
 - (10) Ngai, K. L.; White, T. *Phys. Rev. B.* **1979**, *20*, 2475.
 - (11) Ngai, K. L.; Rajagopal, A. K.; Teiler, S. *Ann. N.Y. Acad. Sci.* **1986**, *84*, 150, 321.
 - (12) Ngai, K. L.; Plazek, D. J. *J. Polym. Sci. Polym. Phys. Ed.* **1986**, *24*, 619.
 - (13) Boese, D.; Kremer, F. *Macromolecules* **1990**, *23*, 820, 1826.
 - (14) Alberdi, J. M.; Alegría, A.; Macho, E.; Colmenero, J. *J. Polym. Sci., Polym. Lett. Ed.* **1986**, *24*, 399.
 - (15) Alberdi, J. M.; Alegría, A.; Macho, E.; Colmenero, J. *Polym. Bull.* **1987**, *18*, 39.
 - (16) Pakula, T.; Geyler, S. *Macromolecules* **1987**, *20*, 2909.
 - (17) Havriliak, S.; Negami, S. *Polymer* **1967**, *8*, 161.
 - (18) Macho, E.; Alegría, A.; Colmenero, J. *Polym. Eng. Sci.* **1987**, *27*, 810.
 - (19) Vogel, H. *Phys. Z.* **1921**, *22*, 645.
 - (20) Fulcher, G. S. *J. Am. Chem. Soc.* **1925**, *8*, 958.
- Registry No.** PH (copolymer), 25068-38-6; PAr (copolymer), 26590-50-1; PAr (SRU), 39281-59-9; PSF (SRU), 25135-51-7; PC (SRU), 24936-68-3; PC (copolymer), 25037-45-0.